

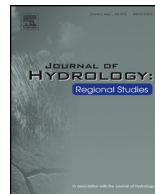


ELSEVIER

Contents lists available at ScienceDirect

## Journal of Hydrology: Regional Studies

journal homepage: [www.elsevier.com/locate/ejrh](http://www.elsevier.com/locate/ejrh)



# Simulating the impact of climate change on the groundwater resources of the Magdalen Islands, Québec, Canada

Jean-Michel Lemieux<sup>a,\*</sup>, Jalil Hassaoui<sup>a</sup>, John Molson<sup>a</sup>, René Therrien<sup>a</sup>, Pierre Therrien<sup>a</sup>, Michel Chouteau<sup>b</sup>, Michel Ouellet<sup>c</sup>

<sup>a</sup> Département de géologie et de génie géologique, Université Laval, 1065 avenue de la Médecine, Québec (Québec) G1V 0A6, Canada

<sup>b</sup> École Polytechnique de Montréal, Département des Génies civil, géologique et des mines, C.P. 6079 Succursale Centre-Ville, Montréal (Québec) H3C 3A7, Canada

<sup>c</sup> Direction de l'aménagement et des eaux souterraines, Direction générale des politiques de l'eau, Ministère du Développement durable, de l'Environnement et de la Lutte contre les changements climatiques, 675, boul. René-Lévesque-Est, 8e étage, bte 42, Québec (Québec) G1R 5V7, Canada

### ARTICLE INFO

#### Article history:

Received 28 May 2014

Received in revised form 16 December 2014

Accepted 18 February 2015

Available online 2 April 2015

#### Keywords:

Coastal aquifers

Seawater intrusion

Climate change

Magdalen Islands

### ABSTRACT

**Study region:** This study is conducted in the Magdalen Islands (Québec, Canada), a small archipelago located in the Gulf of St. Lawrence.

**Study focus:** This work was undertaken to support the design of a long-term groundwater monitoring network and for the sustainable management of groundwater resources. This study relies mostly on the compilation of existing data, but additional field work has also been carried out, allowing for the first time in the Magdalen Islands, direct observation of the depth and shape of the transition zone between freshwater and seawater under natural conditions. Simulations were conducted along a 2D cross-section on Grande Entrée Island in order to assess the individual and combined impacts of sea-level rise, coastal erosion and decreased groundwater recharge on the position of the saltwater–freshwater interface. The simulations were performed considering variable-density flow and solute transport under saturated–unsaturated conditions. The model was driven by observed and projected climate change scenarios to 2040 for the Magdalen Islands.

**New hydrological insights for the region:** The simulation results show that among the three impacts considered, the most important is sea-level rise, followed by decreasing groundwater recharge and coastal erosion. When combined, these impacts cause the saltwater–freshwater interface to migrate inland over a distance of 37 m and to rise by 6.5 m near the coast to 3.1 m further inland, over a 28-year period.

© 2015 The Authors. Published by Elsevier B.V. This is an open access article under the CC BY-NC-ND license (<http://creativecommons.org/licenses/by-nc-nd/4.0/>).

\* Corresponding author. Tel.: +1 418 656 7679.

E-mail addresses: [jmlemieux@ggl.ulaval.ca](mailto:jmlemieux@ggl.ulaval.ca) (J.-M. Lemieux), [jalil.hassaoui@gmail.com](mailto:jalil.hassaoui@gmail.com) (J. Hassaoui), [john.molson@ggl.ulaval.ca](mailto:john.molson@ggl.ulaval.ca) (J. Molson), [rene.therrien@ggl.ulaval.ca](mailto:rene.therrien@ggl.ulaval.ca) (R. Therrien), [pierre.therrien@ggl.ulaval.ca](mailto:pierre.therrien@ggl.ulaval.ca) (P. Therrien), [chouteau@geo.polymtl.ca](mailto:chouteau@geo.polymtl.ca) (M. Chouteau), [michel.ouellet@mddelcc.gouv.qc.ca](mailto:michel.ouellet@mddelcc.gouv.qc.ca) (M. Ouellet).

## 1. Introduction

Sustainable groundwater supply for maritime coastal communities is a constant challenge due to the presence of surrounding seawater and its possible intrusion into freshwater aquifers. This challenge is even greater for island communities where there are no other sources of drinking water. This is the case of the Magdalen Islands, a small archipelago of 200 km<sup>2</sup> located in the Gulf of St. Lawrence in eastern Canada where 13,000 inhabitants depend entirely on groundwater for their potable water supply (Dessureault and Simard, 1970; BAPE, 2013). In this situation, one of the biggest threats for the water supply is the upconing of seawater into the freshwater supply wells. Saltwater upconing is especially serious because high salinity will force a well to be abandoned for a relatively long period as the upconed seawater slowly decays (Zhou et al., 2005). In the long term, this situation may occur due to over-extraction of freshwater in pumping wells or to changes in natural conditions induced by climate change.

While predictions of seawater upconing under various pumping conditions have been extensively studied in the context of water management (e.g. Dagan and Bear, 1968), the impacts of climate change, and more specifically the impact of sea-level rise, on saltwater intrusion has only gained interest recently. Recent studies have been conducted for both confined and unconfined aquifers at either specific sites (e.g. Sherif and Singh, 1999; Bobba, 2002; Green and MacQuarrie, 2014) or generic sites using parametric studies (e.g. Werner and Simmons, 2009; Webb and Howard, 2011; Ferguson and Gleeson, 2012) with a wide range of models including analytical solutions, numerical models using the Ghyben–Herzberg assumption, and fully coupled density-dependent flow and solute transport models.

The reported impacts of sea-level rise are highly variable because they depend on the site hydrogeological context, climate conditions and geometry of the aquifers, as well as on the selected boundary conditions. For instance, Werner and Simmons (2009) and Werner et al. (2012) have shown that flux-controlled systems, in which the groundwater discharge flux to the sea is constant despite the sea-level rise, are much less sensitive to sea-level rise than constant-head systems, where the inland boundary is controlled by groundwater abstraction and where the heads are prescribed. These conclusions are particularly relevant for small island aquifers (Morgan and Werner, 2014).

While sea-level rise is usually considered the main impact of climate change on coastal aquifers, other impacts can also be expected, such as coastal erosion and changes in precipitation and temperature, which may in turn impact evapotranspiration and groundwater recharge. The magnitude of these individual impacts is poorly documented and it is not obvious whether they will have a cumulative effect or will offset each other.

Recently, Green and MacQuarrie (2014) investigated the relative importance of projected sea-level rise, climate change effects on recharge and groundwater extraction rates on seawater intrusion in an unconfined sandstone aquifer located on the coast of the Gulf of St. Lawrence in New Brunswick. Their scenario, investigating the period between 2011 and 2100, is based on a decrease in groundwater recharge (40–85 mm/year), a sea-level rise (0.93–1.86 m) and a pumping rate increase (by a factor of 2.3) for 2100. Although the relative importance of the three factors changes according to the specific location, they found that sea-level rise had the least impact on seawater intrusion into shallow and intermediate aquifers. The effect of declining recharge was most significant at shallow to intermediate depths along the transition zone, while the impact of increased pumping rates was limited to the area close to the well and at the same depth of extraction.

Predicting the dynamics of a freshwater–saltwater interface can also be valuable for designing a groundwater monitoring network as part of a groundwater management strategy. For example, in 2007 the Quebec Ministry of Sustainable Development, Environment and the Fight Against Climate Change (MDDELCC) implemented an action plan on climate change in which Action 22 aims at maintaining a monitoring network to evaluate the impacts of climate change on groundwater resources (Government of Québec, 2008). Because of the specific hydrogeological context of the Magdalen Islands, the monitoring network should allow tracking the position of the freshwater–saltwater interface. Up to now, two different options have been considered for monitoring the interface: time-domain electromagnetic (TDEM) surveys and instrumented boreholes. This study should help to decide whether the expected changes are within the resolution of the TDEM method and if

not, how to design the observation wells and how to choose and configure the various measuring instruments.

In this context, the objective of the study is to quantify the potential impact of climate change on the freshwater resources of the Magdalen Islands. More specifically, we are interested in the individual and cumulative impacts of sea-level rise, erosion and groundwater recharge on the position of the freshwater–saltwater interface. This study will contribute to the sustainable management of groundwater resources in the archipelago and will provide the basis for long-term monitoring of climate changes impacts.

First, the study area is presented, including results from a field campaign where a borehole was drilled across the freshwater–saltwater interface and where groundwater sampling and hydraulic tests were conducted. This is followed by a review of the predicted and observed changes in climate on the Magdalen Islands with specific attention to sea-level rise, erosion, precipitation, temperature, evapotranspiration and groundwater recharge. The selected numerical model is then presented along with the simulation domain, parameters, initial conditions, boundary conditions and simulated scenarios. Individual and combined results pertaining to the impact of sea-level rise, erosion and groundwater recharge are then presented and discussed in order to fully appreciate the expected impact of climate change on groundwater resources.

## 2. Study area

The Magdalen Islands form an archipelago comprising fifteen islands with a land surface of about 200 km<sup>2</sup> located in the heart of the Gulf of St. Lawrence, 205 km south-east of the coast of the Gaspé Peninsula and about 100 km north-east of the provinces of Prince Edward Island and Nova Scotia, Canada (Fig. 1). The population of the archipelago is about 13,000 who mostly inhabit seven of the fifteen islands, which are primarily connected by sand dunes (Fig. 1). The islands Entrée, Havre Aubert, Cap aux Meules, Havre aux Maisons, Loups and Grande Entrée are part of the Municipality of Îles-de-la-Madeleine, while Grosse and Est Islands are part of the Municipality of Grosse-Île.

### 2.1. Geology

The Magdalen Islands are part of the Magdalen Basin, which is a sub-basin of the Upper Paleozoic Maritimes Basin, containing continental and shallow marine strata of Late Devonian–Early Permian age (Dietrich et al., 2011). According to Brisebois (1981) who mapped the area, four stratigraphic units can be identified in the Magdalen Islands, which can be grouped into two assemblies separated by an unconformity. The bottom of the sequence is composed of the Mississippian formations of Havre aux Maisons (terrigenous sediments, carbonates, evaporites) and Cap au Diable (volcanoclastics and basalts). These rocks underlie the central part of the islands of Havre Aubert, Cap aux Meules and Havre aux Maisons and are elevated compared to the rest of these islands because they are more resistant to erosion than the surrounding rocks (Fig. 1). The Mississippian formations are underlain by 5 km thick salt diapirs that lifted the sequence and contributed to the formation of large faults in the area. The upper part of the sequence is composed of the lower Permian formation of Cap-aux-Meules, which is made of two members: Étang-du-Nord (sandstone, conglomerate, mudstone, limestone) and Étang-des-Caps (red sandstone with giant oblique laminations).

These rocks are covered with a discontinuous and mostly thin layer of unconsolidated Quaternary deposits left by the last glacial period. The only important accumulation of unconsolidated sediments is located in the central part of Grande Entrée Island, where their thickness can reach up to 60 m (Sylvestre, 1979). Finally, modern unconsolidated surface sand deposits surround and link most of the islands.

### 2.2. Hydrogeology

Among the above rock units, the red sandstone member of Étang-des-Caps is the most permeable geologic unit from which all municipal wells of the archipelago exploit groundwater. The Étang-du-Nord member is also quite permeable and is extensively used for private wells. The hydraulic

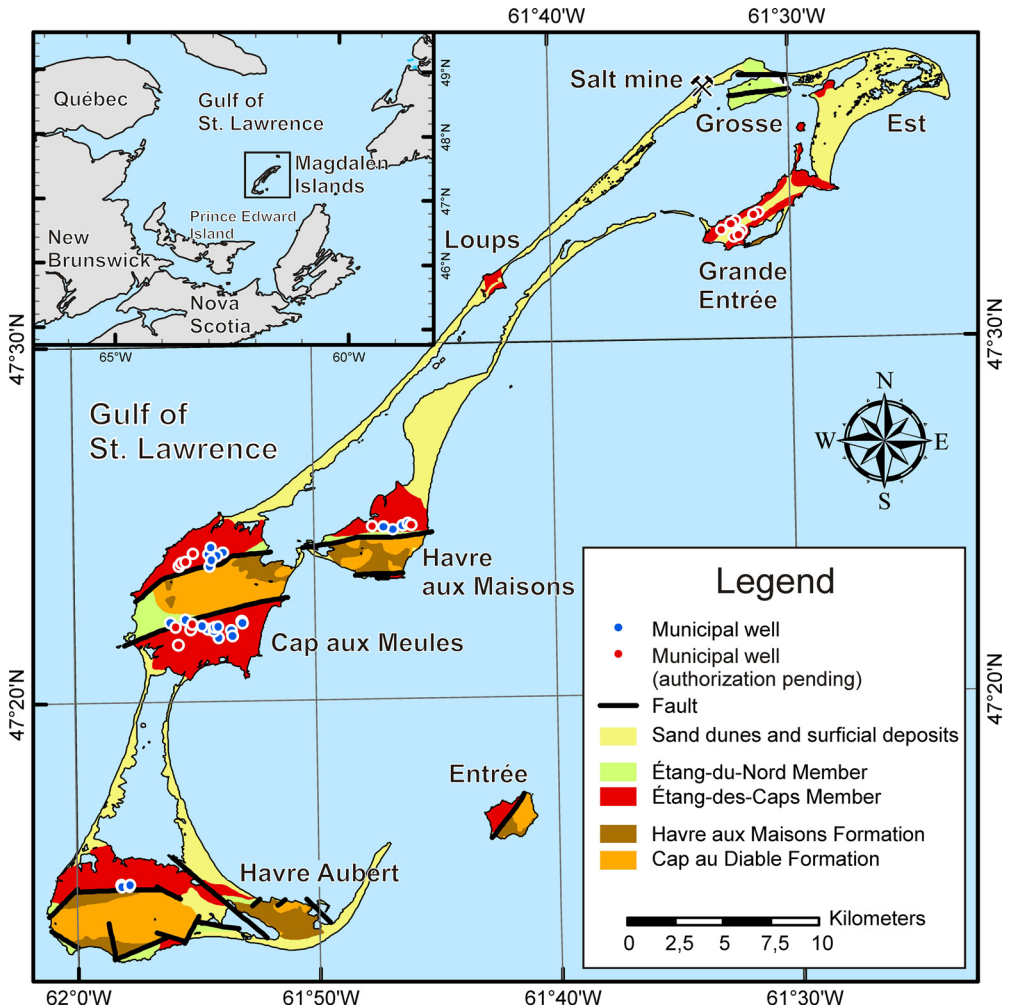


Fig. 1. Geology of the study area indicating current and projected wells for the Municipality of Îles-de-la-Madeleine.

conductivity of the Havre aux Maisons and Cap au Diable formations is very low and these formations are not classified as aquifers (Sylvestre, 1979). Sand dunes are also used for private wells along with providing water for a salt mine located on Grosse Île (Fig. 1).

Because there are no surface water bodies in the archipelago, groundwater is the only available source of fresh water. The municipality of Îles-de-la-Madeleine is the only municipality with a water distribution service. This service relies on 26 groundwater wells located on the islands of Cap aux Meules (18), Havre aux Maisons (4) and Havre Aubert (4). Private wells provide the water supply of the inhabitants of the other islands. To meet the drinking water needs for the next 30 years, the Municipality is currently expanding its network of groundwater wells. Authorization requests have been made to the MDDELCC for the commissioning of 10 new wells on Cap aux Meules Island and nine new wells on Grande Entrée Island to supply a new water distribution network (Fig. 1).

On Grande Entrée Island, where this study was conducted, freshwater was until now supplied from individual private wells. However, a new groundwater well field and a new water supply network were recently constructed and are being progressively put into operation. This well field was designed

to supply 345 m<sup>3</sup>/d of water (Madelin'Eau, 2009). To put these groundwater extraction rates into perspective, the mean groundwater recharge estimates for this island is 4631 m<sup>3</sup>/d (Sylvestre, 1979).

### 2.3. Study site

The site selected for the study is Grande Entrée Island where groundwater is considered most vulnerable to the impact of climate change because the water table is at most only 3 m above sea level. The depth of the freshwater–saltwater interface is also among the shallowest of the archipelago, which poses a major problem for the operation of future wells. The geology of the island is also quite simple as the island is composed of flat-lying red sandstones of the Étang-des-Caps formation overlain by unconsolidated deposits. Finally, the freshwater–saltwater interface is best described for Grande Entrée Island.

The aquifer on this island is composed of highly permeable layered sandstones that have an average hydraulic conductivity of  $1 \times 10^{-4}$  m/s but can span over four orders of magnitude. The layered nature of the rocks suggests anisotropy in the hydraulic conductivity but this parameter has not been quantified. Field observations also indicate that the sandstones are fractured. However, there is no detailed description of the fracture network or the hydraulic properties of the individual fractures. Laboratory measurements conducted on Étang-des-Caps sandstone from the Island of Cap aux Meules shows that its porosity ranges between 28 and 32% (Gélinas and Choquette, 1996). Laboratory experiments with the same samples were conducted in order to determine the capillary properties of the material (Gélinas and Choquette, 1996). These data were adjusted to the Van Genuchten (1980) model to determine the unsaturated parameters of the media. Their adjustment gives values of  $\alpha = 0.72 \text{ m}^{-1}$  and  $n = 2.9$  with a residual water saturation  $S_r = 0.08$ . Reported specific storage estimates from pumping test have an average value of  $5.7 \times 10^{-4} \text{ m}^{-1}$ . Finally, a groundwater recharge value of 220 mm/yr was proposed based on a simple water budget method (Poulin, 1977) and on the analysis of the water-table fluctuations in an observation well (Leblanc, 1994).

Time domain electromagnetic (TDEM) surveys were conducted in 2011 at different locations of the archipelago to infer the depth of the freshwater–saltwater interface (Chouteau et al., 2011) and to verify whether the Ghyben–Herzberg relationship is valid in the Magdalen Islands hydrogeological context. The eight TDEM surveys which were conducted on Grande Entrée Island yielded a depth of the freshwater–saltwater interface between 21.8 m (−19.8 mbsl) and 47.7 m (−36.4 mbsl). A 80 m deep borehole (called the MDDELCC observation well hereafter) was then drilled in 2012 close to one of the TDEM surveys at a depth greater than the inferred depth of the freshwater–saltwater interface to verify the validity of the interpretation of the geophysical survey. Electromagnetic (EM) well logs were performed in the well along with manual readings of water conductivity in the open borehole with a conductivity probe (Fig. 3). Finally, straddle packers were used to sample groundwater and conduct hydraulic conductivity measurements at different depths in the borehole with an interval length of 1.5 m (Fig. 3).

These measurements allowed direct observation of the shape of the transition zone between freshwater and saltwater under natural conditions for the first time on the Magdalen Islands (Fig. 3a and b). Three different profiles are shown in Fig. 3a. Two of the profiles show the TDS concentration measured with a conductivity probe at two different times (October 2012 and 2014) and converted to TDS concentration (g/l) with the following relation (Comte and Banton, 2007):  $\text{TDS} = (\text{EC}/2.211)^{1/0.926}$  where EC is the electrical conductivity (mS/cm). The third profile shows the TDS concentration measured for groundwater samples collected at discrete intervals isolated by the straddle packers.

The TDS profile obtained from the conductivity probe in 2012 is relatively dispersed and smeared (Fig. 3a). Since this profile was obtained only shortly after the borehole was completed, we contend that this conductivity profile has been influenced by vertical water mixing in the well related to the drilling operations and is not representative of natural conditions. It was originally expected that the TDS profile obtained from the water samples collected with the straddle packers would be closer to natural conditions, because they were formation samples. However, even if the shape of the profile is more natural and sharper than the profile obtained with the conductivity probe, the maximum measured TDS was only 21 g/l, which is much less than the concentration measured with the conductivity probe

deeper in the well. This is also much less than expected, since the TDS concentration in this area of the Gulf of St. Lawrence is reported to vary between 29 and 37 g/l (Comte and Banton, 2006). This means that water used during the drilling procedure probably entered the formation and diluted the saltwater within and below the mixing zone. This could explain why the shape of the TDS profile is reasonable, but the TDS values are lower than expected. Fortunately, a recent visit to the site in October 2014 allowed obtaining a new TDS profile with the same conductivity probe. This profile (Fig. 3a), which is considered representative of natural conditions, exhibits a sharp increase in TDS concentration at the same depth as with the straddle packers, but with a higher maximum TDS concentration of 34.1 g/l

Based on this information, the mixing zone between freshwater and saltwater would be located between depths of 35 m to 45 m below ground surface. These observations are also supported by the EM well logs conducted in the borehole where the sudden increase in electric conductivity measured at these depths can be related to an increase in salinity (Fig. 3b). The shape of this profile, which measures conductivity of the rock formation and groundwater within a 1 m radius around the borehole, is more in line with the sharp TDS profile obtained with the groundwater samples and with the conductivity probe from October 2014. Below 45 m, the electric conductivity varies, but these variations are attributed to local changes in porosity.

The interpretation of the TDEM soundings GE01 and GE06 that were conducted within 100 m of the borehole before it was drilled suggests that the transition zone is located at depths of 43.5 m and 47.7 m (Fig. 3c). These results are compatible with the borehole observations, and the small differences in the depth of the mixing zone are related to the difference in elevation between the well and the TDEM survey sites and the fact that the site elevations were not surveyed but inferred from a digital elevation model.

Finally, slug test results are shown in Fig. 3d. The hydraulic conductivity values range between  $3 \times 10^{-6}$  and  $3 \times 10^{-5}$  m/s. These values compare well with those reported for the surrounding wells but are less than the average value for the island. This is probably due to the short interval length used for the slug tests (1.5 m), whereas most of the reported values are for pumping tests investigating larger volumes of rock, which would intercept more fractures.

### 3. Observed and predicted climate change impacts on the Magdalen Islands

Climate change can be defined as a difference of climate conditions over a given period, with respect to a reference period, due to natural or anthropogenic causes (Environment Canada, 2014). The Intergovernmental Panel on Climate Change (IPCC) Fourth Assessment Report (IPCC, 2007) underlines that warming of the climate system is unequivocal, as is now evident from observations of increases in global average air and ocean temperatures, widespread melting of snow and ice and rising global average sea levels.

In the future, climate change may also impact the equilibrium between freshwater and saltwater in coastal aquifers. Sea-level rise, coastal erosion and groundwater recharge variations are the principal consequences of climate change considered in this paper for which observations and predictions are presented below. Because one of the scenarios involved future changes in groundwater recharge, a water budget based on predictions of temperature and precipitation is also presented.

#### 3.1. Sea-level rise

The average global sea level has risen by about 140 mm between 1950 and 2010 mainly due to the melting of glaciers and thermal expansion of the oceans (Stammer et al., 2013). According to the IPCC, the average predicted sea-level rise for 2100 is between 0.26 m and 0.97 m, while worst-case projections reach 1.80 m (Vermeer and Rahmstorf, 2009). However, on the Magdalen Islands, the relative sea-level rise is accentuated by regional subsidence due to a forebulge collapse linked to the last glacial period (Koozhare et al., 2008). Tide gage analysis for the Cap-aux-Meules station shows that the combination of these two phenomena has resulted in a relative sea-level rise of about 3.5 mm/yr since 1960 (Fig. 4). These results are in close agreement with those obtained on Prince Edward Island (Forbes et al., 2004) where the sea-level rise was estimated with tide-gauge records to be 3.2 mm/yr since 1911. They also projected that the relative sea-level rise for 2100 should be

**Table 1**

The four scenario families of the Fourth IPCC Assessment Report with their respective global average surface warming projections to 2100 (IPCC, 2007).

	More economic focus	More environmental focus
Globalisation	<b>A1</b> Rapid economic growth (groups: A1T; A1B; A1FI) <b>1.4–6.4 °C</b>	<b>B1</b> Global environmental sustainability <b>1.1–2.9 °C</b>
Regionalization	<b>A2</b> Regionally oriented economic development <b>2.0–5.4 °C</b>	<b>B2</b> Local environmental sustainability <b>1.4–3.8 °C</b>

0.7 m ± 0.4 m. Similar forecasts are available for New Brunswick where, depending on the location, predicted relative sea-level rise is expected to be in the range from 0.9 to 1.0 m ± 0.38 m for 2100 (Daigle, 2011).

### 3.2. Erosion

Erosion is an important concern for the small archipelago of the Magdalen Islands, especially on Havre Aubert and Cap aux Meules Islands along with the Pointe aux Loups area where sandstone cliffs, tombolos and sand dunes are sensitive to freeze-thaw cycles, wave wash-overs and strong winds (Bernatchez et al., 2008). Coastal recession rates of 0.79 m/yr were observed for the Pointe aux Loups area for the 1963–2001 period while rates of 0.46 m/yr, 0.31 m/yr and 0.09 m/yr were observed for sandstone cliffs, sand beaches and sand dunes of the Havre Aubert and Cap aux Meules Islands (Bernatchez et al., 2008). The predicted coastal withdrawal for 2050 is close to 38 m for the Cap aux Meules Island, which corresponds to a rate of 0.77 m/yr (Bernatchez et al., 2008). These values are quite high due to the soft nature of the rocks. No predictions are available for the Grande Entrée study area.

### 3.3. Temperature and precipitation

The analysis of mean annual temperature and total annual precipitation from the Cap-aux-Meules weather station (operational since 1985) shows a respective increase of 0.09 °C/yr and 1.6 mm/yr for the 1985–2006 period (Bernatchez et al., 2008). The 2050 forecast for the Maritimes is also an increase in temperature and rainfall (Vasseur and Catto, 2008). According to Bernatchez et al. (2008) this increase will contribute to increased winter thaws and disappearance of snowfall on the Magdalen Islands for the 2041–2070 period. Apart from the predictions of Bernatchez et al. (2008), no specific data are available for the Magdalen Islands in terms of future temperature and precipitation. Because they are required for forecasting groundwater recharge (see next section), specific predictions have been performed in the course of this study.

Air temperatures and precipitation rates were predicted from global climate models (GCM). To capture uncertainty in the predictions, our forecasts consider various emission scenarios and are conducted with several GCMs. The selected emission scenarios are the A1B, A2 and B1 of the IPCC Fourth Assessment Report (IPCC, 2007) for which the Canadian Climate Change Scenarios Network (CCCSN) provides monthly temperature and precipitation forecasts from 2010 to 2100 for 24 different GCMs (see Environment Canada, 2014 for details; Table 1).

Moreover, because GCMs have a coarse resolution and are affected by biases between simulated and observed meteorological variables (Van Roosmalen et al., 2007), their predictions cannot be readily used in regional hydrogeological studies and downscaling is required. In this study, the delta change downscaling method was used to convert the regional meteorological outputs (temperature and precipitations) to local meaningful values because it is a simple method that requires a minimum of data.

In the delta change method, GCMs are used for the simulation of temperature and precipitation for a reference control period and for future periods affected by various climate change scenarios. The difference or ratio between the future scenarios and control period is named the delta change factor, which is used to compute temperature and precipitation predictions from observations on the control period. For example, the predicted monthly precipitation averages  $\bar{P}_\Delta$  for the 2013–2040 period are given as the product of the delta change factor for precipitation  $\Delta_p$  and the average observations for the control period  $\bar{P}_{obs}$  (1985–2012):

$$\bar{P}_\Delta(i) = \Delta_p(i) \times \bar{P}_{obs}(i) \quad i = 1, \dots, 12 \quad (1)$$

where  $i$  accounts for the 12 months of the year. The delta change factor for precipitation is calculated as the ratio of the simulated monthly precipitation averages  $\bar{P}_{scen}$  from the GCM scenarios A2, A1B and B1 (2013–2040) over the simulated monthly precipitation averages for the control period (1985–2012):

$$\Delta_p(i) = \frac{\bar{P}_{scen}(i)}{\bar{P}_{cont}(i)} \quad i = 1, \dots, 12 \quad (2)$$

For temperature, the predicted monthly average  $\bar{T}_\Delta$  for 2013–2040 is given by

$$\bar{T}_\Delta(i) = \bar{T}_{obs}(i) + \Delta_T(i) \quad i = 1, \dots, 12 \quad (3)$$

where  $\bar{T}_{obs}$  are the average temperatures for the control period and  $\Delta_T$  is the delta change factor for temperature given by

$$\Delta_T(i) = \bar{T}_{scen}(i) - \bar{T}_{cont}(i) \quad i = 1, \dots, 12 \quad (4)$$

The observed data (temperature and precipitation) are obtained from the Environment Canada Havre-aux-Maisons airport station (#71709) and are assumed representative of the climate conditions observed over the entire archipelago. At this station, complete meteorological data cover the 1985–2012 period (28 years). Observed temperatures and precipitation for the control period, as well as delta change factors for temperature and precipitation for the A1B, A2 and B1 scenarios, are presented in Table 2.

### 3.4. Groundwater recharge predictions

Although groundwater recharge has been estimated for the Magdalen Islands, forecast values are not available. To forecast recharge, the water budget method presented by Thornthwaite and Mather (1955) is used. Because this method is simple and requires only measurements of air temperature and precipitation, it is well suited to forecast recharge using the GCMs predictions presented in the previous section.

In the Thornthwaite and Mather (1955) method, the following equation is solved on a monthly basis:

$$P = ET + \Delta S + R \quad (5)$$

where  $P$  is precipitation,  $ET$  is evapotranspiration,  $\Delta S$  are changes in water storage and  $R$  is surface runoff. Water storage ( $S$ ) can be defined as the sum of soil water storage  $S_s$  and groundwater storage  $S_g$ . It is assumed that evapotranspiration from groundwater storage is negligible, so  $\Delta S_g$  can only be positive and corresponds to the amount of water available for recharge. Soil water storage is assumed to have a maximum value  $S_s^{max}$  that was set at 100 mm as suggested by Thornthwaite and Mather (1955). Runoff is specified as a fraction of precipitation. Here, it is assumed that 40% of precipitation is direct runoff based on the topography and land cover of the island.  $ET$ ,  $\Delta S_s$ , and  $\Delta S_g$  are evaluated as a book keeping procedure based on potential evapotranspiration ( $PET$ ), which is evaluated with the Thornthwaite (1948) method ( $PET = 0$  when the monthly mean temperature is below  $0^\circ\text{C}$ ). For each month, if  $P$  is greater than  $PET$ , then  $ET$  is set to  $PET$ , and the excess precipitation is added to  $S_s$ . If  $S_s$  exceeds  $S_s^{max}$ ,  $S_s$  is set to  $S_s^{max}$  and the remaining excess water is added to groundwater storage (Healy, 2010). This procedure does not account for water storage in the snowpack during winter and considers



**Table 2**

Average observed temperature and precipitation for the control period (1985–2012) as well as monthly absolute change factors for temperature  $\Delta_T$  and relative change factors for precipitation  $\Delta_p$  for the A1B, A2 and B1 scenarios. Delta change factors are averages of the 24 GCMs considered in the CCCSN.

Month	$\bar{T}_{obs}$ (°C)	$\Delta_T$			$\bar{T}_\Delta$ (°C)			$\bar{P}_{obs}$ (mm/yr)	$\Delta_p$			$\bar{P}_\Delta$ (mm/yr)		
		A1B	A2	B1	A1B	A2	B1		A1B	A2	B1	A1B	A2	B1
January	−5.8	1.33	1.04	1.56	−4.4	−4.7	−4.2	94	1.03	1.02	0.96	97	96	90
February	−7.0	1.44	0.80	1.71	−5.6	−6.2	−5.3	72	1.06	1.05	1.03	76	75	74
March	−3.5	1.22	0.72	1.41	−2.3	−2.8	−2.1	77	1.06	1.03	1.01	81	79	77
April	1.6	0.86	0.52	1.03	2.5	2.1	2.6	74	1.04	1.01	0.98	77	74	72
May	7.2	0.80	0.47	0.93	8.0	7.7	8.1	83	1.04	1.04	1.02	86	86	84
June	12.5	0.80	0.48	0.96	13.3	13.0	13.5	77	1.04	1.03	1.03	80	79	79
July	17.5	0.89	0.59	1.14	18.4	18.1	18.7	79	1.00	0.98	1.01	79	78	80
August	18.1	1.02	0.69	1.17	19.2	18.8	19.3	87	1.02	0.99	1.00	89	86	87
September	14.3	0.98	0.76	1.17	15.2	15.0	15.4	95	0.99	1.03	0.96	94	98	91
October	8.7	0.94	0.74	1.22	9.6	9.4	9.9	105	0.98	1.01	0.94	102	106	98
November	3.5	0.93	0.84	1.23	4.4	4.3	4.7	103	1.04	1.04	1.00	107	107	103
December	−1.7	1.02	0.70	1.44	−0.7	−1.0	−0.3	107	1.04	1.04	1.00	112	111	107
<b>Total/average</b>	5.4	1.02	0.70	1.25	6.5	6.1	6.79	1053	1.03	1.02	1.00	1081	1076	1046

**Table 3**

Water budget components for the 2013–2040 period for emission scenarios A1B, A2 and B1. The average recharge  $\Delta S_{avg}$  is the average value obtained with the water budget conducted with 24 GCMs predictions for temperature and precipitation.  $\Delta S_{min}$  and  $\Delta S_{max}$  are the minimum and maximum groundwater recharge values.

Scenario		$P$ (mm/yr)	$R$ (mm/yr)	$ET$ (mm/yr)	$\Delta S$ (mm/yr)
Control period		1053	421	422	209
A1B	$\Delta S_{min}$	1056	422	455	185
	$\Delta S_{avg}$	1081	432	422	229
	$\Delta S_{max}$	1159	464	435	263
A2	$\Delta S_{min}$	1020	408	410	208
	$\Delta S_{avg}$	1076	431	418	231
	$\Delta S_{max}$	1160	464	436	261
B1	$\Delta S_{min}$	789	316	336	151
	$\Delta S_{avg}$	1046	419	421	211
	$\Delta S_{max}$	1111	445	422	247

snow precipitation as liquid precipitation available for recharge. Although this simplification may have a major impact on recharge timing, it is considered acceptable on an annual long-term basis.

The water budget was calculated with the temperature and precipitation predictions from the 24 GCM models used in the CCCSM for the climate change scenarios A1B, A2 and B1. The components of the water budget for the minimum, average and maximum recharge values obtained for each scenario are shown in Table 3. The components of the water budget for the control period are also shown in this table as a reference.

The recharge value obtained for the control period (209 mm/yr) compares well with the recharge estimates (220 mm/yr) from the literature that were presented in Section 2.3. The mean recharge predictions for the 2013–2040 period are 229, 231 and 211 mm/yr for the A1B, A2 and B1 scenarios. These values are only slightly above the value for the control period, which suggests that groundwater recharge should slightly increase as a response to climate change. On the other hand, average evapotranspiration is expected to remain constant. However, if extreme temperature and precipitation predictions from the GCMs are used, significant variability can be expected for groundwater recharge. For example, groundwater recharge could be as low as 151 mm/yr and as high as 263 mm/yr.

## 4. Methods

In this section, the methods used for simulating the impact of climate change on the freshwater–saltwater interface are described. The simulations were performed with the finite-element model FEFLOW V6.1 (DHI-WASY, 2013), which allows the simulation of variably saturated and density-dependent groundwater flow along with solute transport in 2D and 3D. The conceptual model for groundwater flow at the study site on Grande Entrée Island is first presented, followed by the spatial discretization, boundary conditions, and the aquifer and fluid properties. Finally, the simulation strategy is presented.

### 4.1. Conceptual model

Because of the simple hydrogeological context and symmetrical geometry of Grande Entrée Island, density-dependent flow was simulated along a vertical 2D cross section. The cross-section is oriented in the general direction of groundwater flow, which is perpendicular to the coast (Fig. 2) and includes the MDDELCC observation well where the salinity profile was measured.

The conceptual model for groundwater flow and solute transport along the cross-section is shown in Fig. 5. The model extends into the ocean as the freshwater–saltwater interface location is not known a priori and may be located under the sea. We assumed that the center of the island, where the ground elevation is highest, is a groundwater divide. Using this assumption and the fact that the island is symmetric, only half of the island section is considered for the simulations.

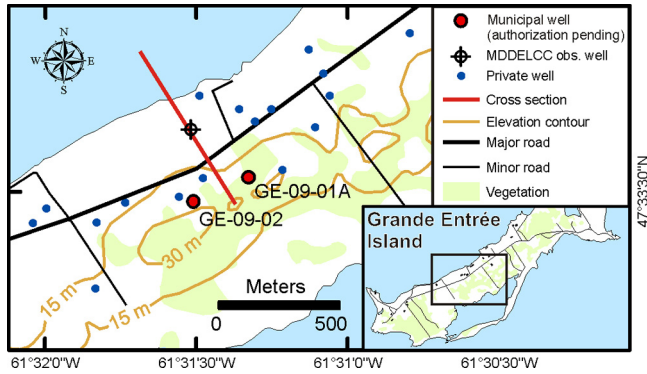


Fig. 2. Location of the cross-section on Grande Entrée Island.

In the conceptual model, only the Étang-des-Caps aquifer is considered. Although a valley filled with up to 60 m of unconsolidated deposits is located at the center of the island (Sylvestre, 1979), it has not been represented because the nature and properties of these deposits are poorly known. Moreover, the Étang-des-Caps aquifer is represented as an equivalent porous medium, although it is known to contain fractures. This choice is mostly made due to the lack of information on fracture properties, but is supported by the high hydraulic conductivity and porosity of the rock matrix that will contribute to minimize the importance of fracture flow and will promote matrix diffusion (e.g. Tang et al., 1981). Therefore, the model can be considered a simplified representation of the study site. This representation is supported by the purpose of the study, which is to assess the dynamics of groundwater flow under a changing climate rather than to exactly match field conditions. The aquifer properties are further assumed to be homogeneous along the cross-section.

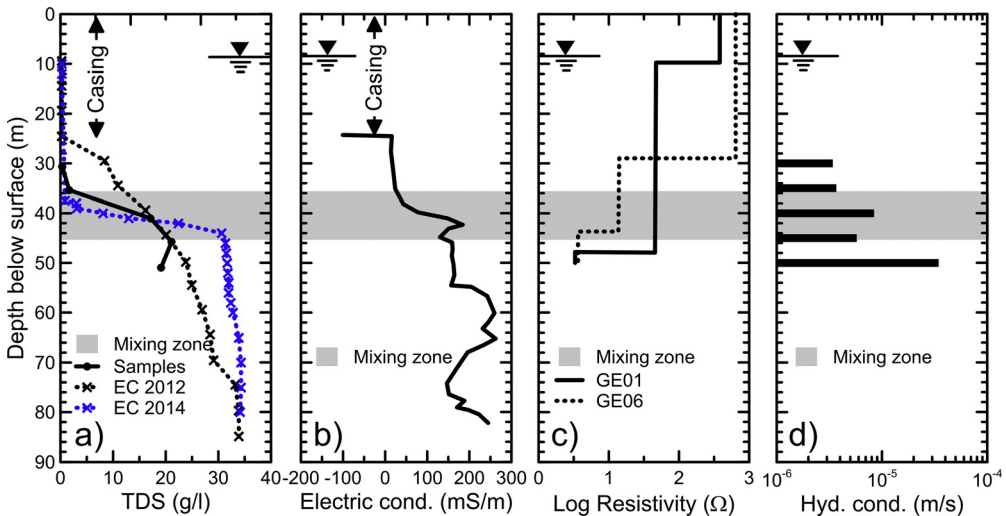
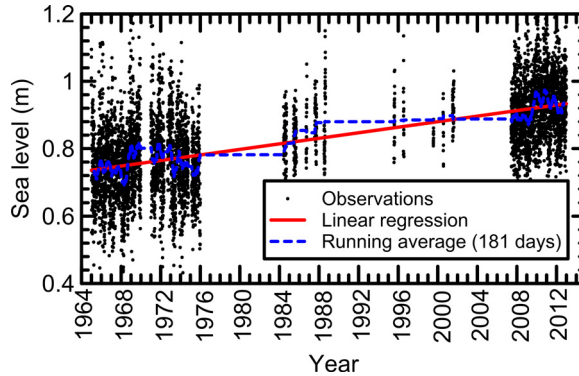


Fig. 3. (a) Measured TDS concentrations in the MDDELCC observation well using the conductivity probe and from the water samples collected with the straddle packers. (b) Electric conductivity well log conducted in the MDDELCC observation well. (c) TDEM surveys conducted close to the MDDELCC observation well. (d) Hydraulic conductivity values measured with slug tests in discrete intervals with the straddle packers in the MDDELCC observation well. In these figures, the interpreted location of the mixing zone between freshwater and saltwater is shown along with the position of the water table. Surface elevation was not surveyed but is about 10 masl.



**Fig. 4.** Daily tide gage measurements at station 1970 of Cap-aux-Meules, Magdalen Islands, with a linear regression and a biannual running average.  
Source of data: [Fisheries and Oceans Canada \(2014\)](#).

Since the studied aquifer is unconfined, groundwater flow in the unsaturated zone was included to track the position of the water table. While there are simpler and numerically less demanding approaches for representing the water table such as surface mesh deformation, unsaturated flow is the only option available in FEFLOW for 2D cross-section simulations. In the saturated and unsaturated zones, groundwater flow is affected by the density of the water, which depends on the concentration of total dissolved solids (TDS) which is simulated here using the advection-dispersion equation.

#### 4.2. Spatial discretization

The simulation domain has a length of 755 m and a maximum height of 229 m (Fig. 6). The top elevation of the model corresponds to the 1:20,000 digital elevation model of the archipelago combined with a bathymetric survey. The bottom of the model is set at a depth of 200 m below sea level, which is shallower than the bottom of the aquifer but significantly deeper than the freshwater–saltwater interface. Because most of the flow occurs in the freshwater portion of the aquifer and in the mixing zone, the location of the bottom of the model is assumed deep enough such that it has little impact on the simulations.

The simulation domain is discretized with 162,128 triangular elements (81,729 nodes), with a higher density of nodes close to the freshwater exit area where computed water fluxes need to be more accurate because the transport boundary condition may change with time depending on the

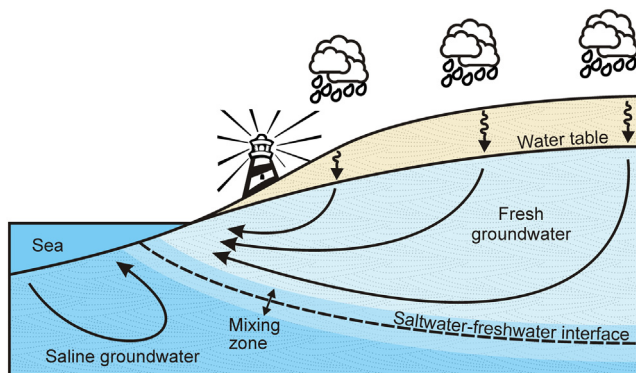


**Fig. 5.** Conceptual model for groundwater flow on Grande-Entrée Island.

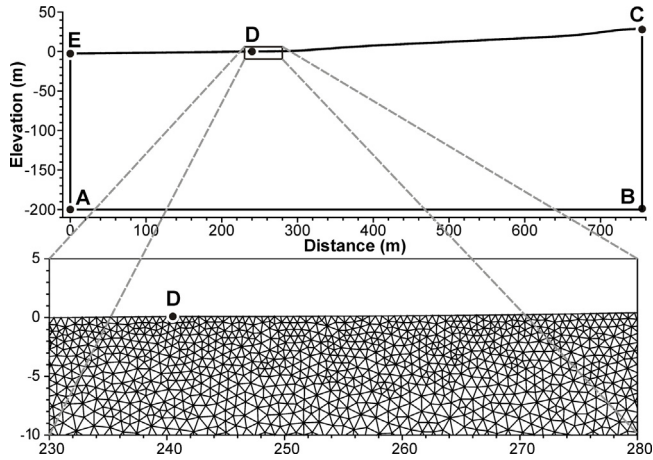


Fig. 6. Simulation domain (ABCDE) showing the spatial discretization. The point D indicates the location of the shoreline.

direction of the water flux (see Section 4.3). The element size varies between 0.7 m and 2 m and the mesh respects the Delaunay criterion (Fig. 6).

4.3. Boundary conditions

The flow and transport boundary conditions are shown in Table 4. The aquifer bottom (AB in Fig. 6) is an impervious boundary for flow and transport. The seaside boundaries AE and ED are assumed to be at seawater hydrostatic pressure. On these boundaries, we specify the saltwater heads ( $h_{sw}$ ) which the model automatically converts to equivalent hydraulic heads  $h$  with:

$$h = h_{sw} + \gamma(h_{sw} - z)$$

where  $\gamma = \rho_{max}/\rho_0 - 1$  and where  $\rho_{max}$  is the density of seawater and  $\rho_0$  is the density of freshwater. The saltwater head is fixed at 200.1 m on boundaries AE and ED because the local sea level is 0.1 m above mean sea level and the datum of the model is set 200 below mean sea level. For transport, a prescribed concentration equal to saltwater TDS (35 g/l) is specified at the seaside boundary (AB). On the sea bed (ED), a mixed-type boundary condition is used depending on the direction of the groundwater flux as suggested by Bear and Cheng (2010). When the water flux is toward the aquifer, a prescribed concentration equal to saltwater TDS (35 g/l) is used but switches to a zero dispersive flux when water flows out of the aquifer toward the sea.

Over the land surface (DC), a specified flux is applied as a recharge boundary condition with a prescribed TDS concentration of 0 g/l. The lateral inland boundary (BC) is a symmetric boundary, which is impervious for flow and transport.

Table 4  
Boundary conditions for the numerical model (boundary limits are shown in Fig. 6).

Boundary	Boundary conditions	
	Flow	Transport
Aquifer bottom (AB)	$q_n = 0$	$\nabla C = 0$
Groundwater divide (BC)	$q_n = 0$	$\nabla C = 0$
Land surface (DC)	$q_n = 220 \text{ mm/y}$	$C = 0$
Seaside (AE)	$h_{sw} = 200.1 \text{ m}$	$C = 35 \text{ g/l}$
Sea bed (ED)		
if $q_n > 0$ (inflow)	$h_{sw} = 200.1 \text{ m}$	$C = 35 \text{ g/l}$
if $q_n < 0$ (outflow)	$h_{sw} = 200.1 \text{ m}$	$\nabla C = 0$

**Table 5**  
Initial and calibrated aquifer properties used in the numerical model.

Parameter	Initial value	Calibrated value
Hydraulic conductivity (m/s)		
Vertical	$1 \times 10^{-4}$	$7 \times 10^{-5}$
Horizontal	$1 \times 10^{-5}$	$7 \times 10^{-6}$
Porosity	0.30	0.30
Specific storage ( $m^{-1}$ )	$1 \times 10^{-4}$	$1 \times 10^{-4}$
Dispersivity (m)		
Longitudinal	50	10
Transverse	0.5	0.08
Van-Genuchten parameters		
$\alpha$ ( $m^{-1}$ )	0.7	0.7
$n$	2.9	2.9

#### 4.4. Aquifer and fluid properties

Aquifer properties initially assigned in the model are shown in Table 5. These values were obtained from observations and measurements reported in the literature, as described in Sections 2.2 and 2.3. Although the aquifer is slightly heterogeneous at the regional scale, it is considered as an unconfined homogeneous anisotropic aquifer with a hydraulic conductivity of  $1 \times 10^{-4}$  m/s, a porosity of 0.3 and an anisotropy factor of 10 ( $K_h/K_v$ ). The longitudinal and transverse dispersivities were initially set to 50 m and 0.5 m. The van Genuchten model is used to relate pressure and saturation in the unsaturated zone, with values of  $0.7 m^{-1}$  and 2.9 for parameters  $\alpha$  and  $n$ , a residual water saturation of 0.08 and a specific storage of  $1 \times 10^{-4} m^{-1}$ . The density of seawater  $\rho_{max}$  is set to  $1.025 g/cm^3$  for a TDS concentration of 35 g/l while the density of freshwater  $\rho_0$  is set to  $1 g/cm^3$  (0 g/l TDS).

#### 4.5. Simulation strategy

Present-day conditions were first simulated by calibrating the model described in the previous section with field observations. The simulated present-day conditions (TDS and heads) were then used as initial conditions for the climate change scenarios. Individual simulations pertaining to the impact of sea-level rise, erosion and groundwater recharge were first conducted, followed by a simulation combining these three impacts. Each of these simulations was run under transient conditions for a period of 28 years (2013–2040) with a time step of 1 day, which satisfies the Courant stability criterion.

Three fictitious observation wells (OW1, OW2 and OW3), located respectively at 50 m, 150 m and 350 m from the shoreline, were specified in the model to observe the impacts of climate change. The MDDELCC observation well was also set in the model at a distance of 250 m from the coast.

##### 4.5.1. Sea-level rise

For the sea-level rise simulation, the surface boundary conditions were modified to account for the progressive inland displacement of the sea shore. Fig. 7a is a schematic representation of the surface boundary condition evolution where the sea shore (D) is displaced progressively inland (D'). In the model, the location of D' is updated every five years and all surface nodes along the ED' boundary are set as prescribed heads with the mixed transport condition described in Section 4.3. At the same time, all surface elements on the new D'C boundary are set to a specified recharge condition with a prescribed freshwater TDS concentration.

Nodes and boundary conditions affected by the imposed sea-level rise are updated six times during the simulation period. This means that six successive simulations were conducted, each of which used results from the previous simulation as the initial condition. A constant rate of sea-level rise of 0.7 mm/yr was selected, as proposed by Forbes et al. (2004) for Prince Edward Island. Sea-level elevation and prescribed heads with time for the AE and ED' boundaries are presented in Table 6.

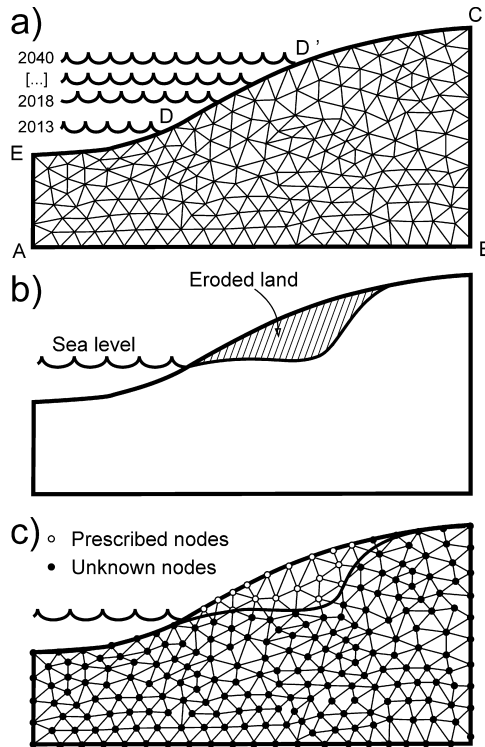


**Fig. 7.** (a) Schematic surface boundary condition evolution for the sea-level rise simulation. (b) Schematic prescribed node assignment for the erosion simulation. (c) The nodes in the eroded portion of the mesh are prescribed while the remaining nodes are unknowns. The diagrams are not to scale and are vertically exaggerated.

#### 4.5.2. Coastal erosion

Coastal erosion options are not provided in the FEFLOW model. While a good option to handle coastal erosion would be to render eroded elements as inactive, inactive elements were not available in the version used. Therefore, we have selected a simple approach where the nodes of the eroded elements are converted to specified heads equal to sea-level elevation and assigned a specified seawater TDS concentration. This approach is shown conceptually in Fig. 7b and c.

Based on erosion rates observed elsewhere in the archipelago (see Section 3.2), an erosion rate of 0.77 m/yr was selected. This value may be higher than erosion rates for Grande Entrée Island but can be considered as the worst-case scenario. Boundary conditions were updated every five years, which corresponds to a total erosion distance of 3.85 m ( $5 \times 0.77$  m/yr). Again, successive simulations were conducted, each of them using results of the previous simulation as the initial condition.

**Table 6**

Prescribed saltwater head on the AE and ED' boundaries for the sea-level rise simulation.

Time period (yr)	Relative sea level (m)	Prescribed saltwater head on AE and ED' (m)
2013	0.0	200.1
2013–2018	0.036	200.136
2018–2023	0.078	200.178
2023–2028	0.124	200.124
2028–2033	0.159	200.159
2033–2038	0.194	200.194
2038–2040	0.215	200.315

#### 4.5.3. Groundwater recharge

Mean predicted groundwater recharge rates from the water balance model presented in Section 3.4 for each climate scenario are similar to the present-day calculated value of 220 mm/yr (Table 3). Since mean recharge is not predicted to change, there would be no future impact for simulations based on these values. Therefore, the worst-case prediction, which yielded a lower groundwater recharge rate of 151 mm/yr for 2040, was selected instead as an extreme case. In the model, groundwater recharge is decreased linearly from present-day conditions (220 mm/yr in 2013) to the predicted value for 2040 (151 mm/yr).

#### 4.5.4. Combined impacts

In the future, it is more likely that the impact of sea-level rise, coastal erosion and decreased groundwater recharge will occur simultaneously rather than independently. Therefore, a simulation combining these three impacts was also conducted. As was done for the erosion and sea-level rise scenarios, the boundary conditions are specified manually and updated every five years, using the results of the previous simulation as the initial conditions for the following period. The rates of sea-level rise, erosion and recharge are the same as for the individual simulations presented in the previous sections.

For each simulation period, specified heads are assigned first for the nodes below sea level. The position of the shoreline is then evaluated. The eroded portion of the mesh is then identified and those nodes affected by erosion are assigned a specified head equal to the corresponding sea-level elevation at that time. The remaining surface boundary elements between the specified heads and inland model boundary are given a uniform recharge rate.

## 5. Results

In this section, the calibration for the present-day model is first presented. Then, results pertaining to the simulation of the individual impacts of sea-level rise, coastal erosion and decreased groundwater recharge are shown. Finally, results are presented for the simulation where the combined impacts are considered. For discussion purposes, the 17.5 g/l TDS isocontour, which correspond to  $C/C_0 = 0.5$ , is considered as the position of the freshwater–saltwater interface.

### 5.1. Present-day conditions

The model was first calibrated assuming steady-state conditions for flow and transport with the boundary conditions shown in Table 4. Calibration was done manually by changing the initial dispersivity and hydraulic conductivity values reported in Table 5 until the model reproduced the best possible shape of the concentration profile in the MDDELCC observation well along with water levels in surrounding wells. The profile shown in Fig. 8b is the best fit and was obtained with a horizontal hydraulic conductivity of  $7 \times 10^{-5}$  m/s, a vertical hydraulic conductivity of  $7 \times 10^{-6}$  m/s and longitudinal and transverse dispersivities of 10 m and 0.08 m, respectively (Table 5). The calibrated hydraulic conductivities are very close to the maximum value measured in the field ( $3 \times 10^{-5}$  m/s), and while no independent measurements of dispersivity were available to compare with, the chosen values are consistent with the system scale (ex. Schulze-Makuch, 2005; Gelhar and Axness, 1983).

The spatial distribution of the TDS concentrations for the calibrated present-day model is shown in Fig. 8a where the location of the observation wells is shown. Freshwater is shown in blue and saltwater in red. The transition zone is rather sharp and located at a maximum depth of about 50 m below sea level.

The simulated water level at a distance of 450 m from the coast is 0.93 m while the water level measured at a nearby well (GE-09-01A) located at the same distance from the coast (Fig. 2) is 1.31 m. No comparison could be made for the MDDELCC observation well because it was not surveyed and the precision of the estimated water level is too low. Considering the natural heterogeneity of the site and the fact that the MDDELCC well was not surveyed, we consider that the calibrated model is suitable for conducting the climate change simulations.



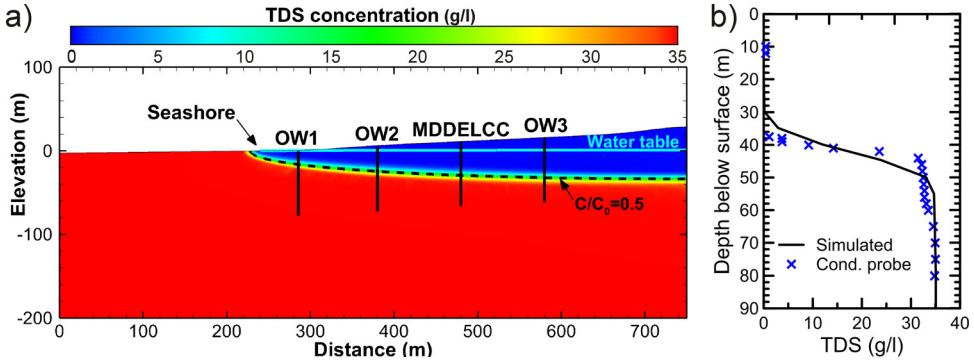


**Fig. 8.** (a) Simulated TDS concentrations for the present-day scenario. (b) Simulated and observed TDS with depth at the location of the MDDELCC observation well.

5.2. Sea-level rise

The TDS concentrations simulated for 2040 for the sea-level rise scenario, shown in Fig. 9a, indicate that the freshwater–saltwater interface would move laterally over a distance of 36 m between 2013 and 2040. At the MDDELCC observation well, the interface would rise by 1.7 m over the period 2013–2040 (see Fig. 10). The rise of the interface would be greater near the coast (Fig. 10a) than toward the center of the island (Fig. 10d). For example, the interface would rise by 5.5 m at OW1 located 50 m from the coast, while it would rise by 1.3 m at OW3 located 450 from the coast. A summary of the predicted rise of the freshwater–saltwater interface shown in Fig. 10 is given in Table 7 for every simulation and for each observation well.

The simulations indicated that there is a long delay between the time sea level rises and the time required for the freshwater–saltwater interface to reach a new equilibrium position. As a result, the location of the interface at the end of the simulation period presented above, for year 2040, is lower

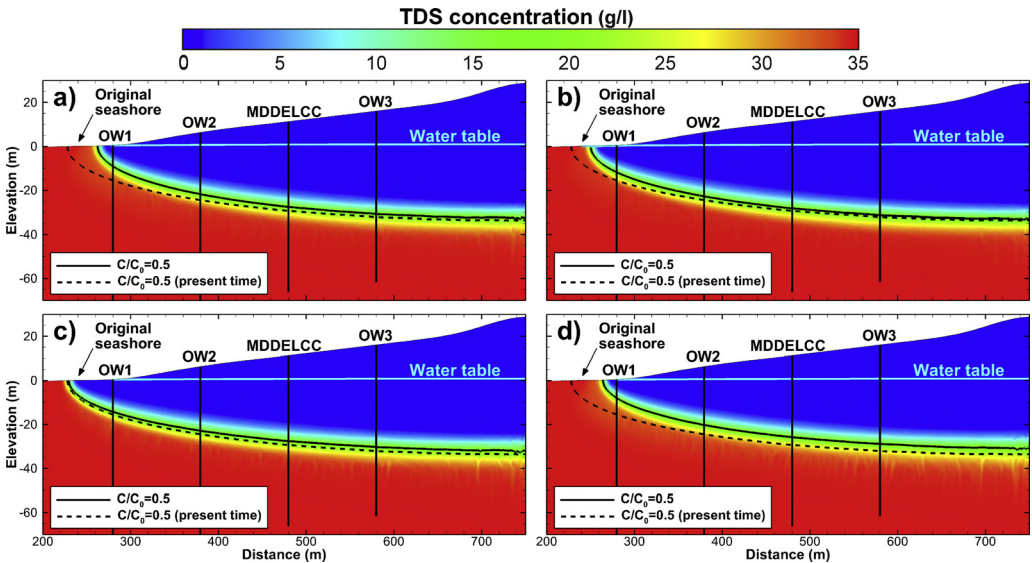


**Fig. 9.** Simulated TDS concentrations for 2040 for the individual impacts of (a) sea-level rise, (b) coastal erosion, (c) groundwater recharge decrease. (d) Combined impacts. Vertical exaggeration: 2.5.

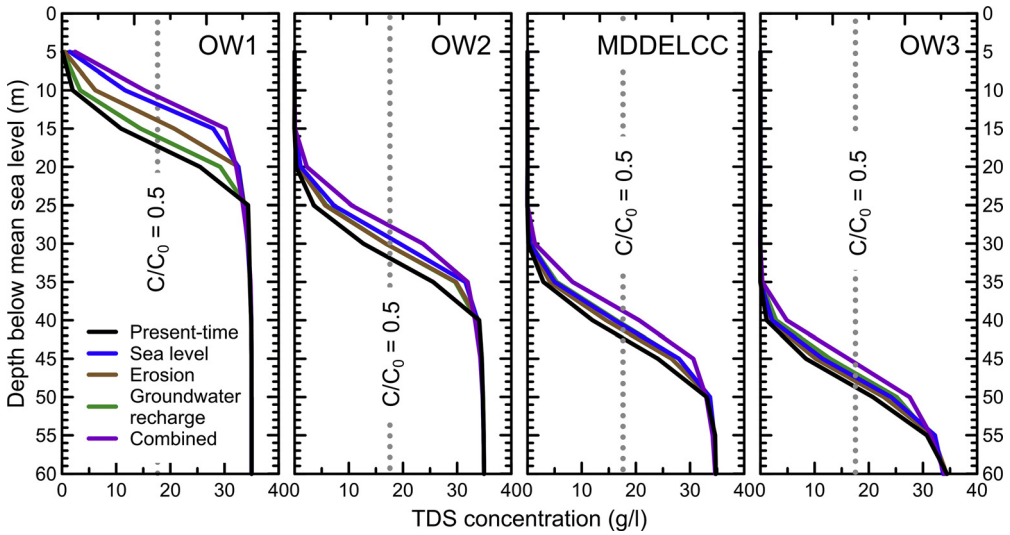


**Fig. 10.** TDS concentration with depth for 2040 for the four observation wells OW1, OW2, MDDELCC and OW3 which are respectively located at a distance of 50 m, 150 m, 250 m and 350 m from the shore. For each graph, the profile is given for the present-time simulation along with the individual and combined impact of climates changes related to sea-level rise, coastal erosion and groundwater recharge. The dotted line indicates the position of  $C/C_0 = 0.5$ , which is considered as the position of the freshwater–saltwater interface.

than its equilibrium position for the prescribed sea level rise. To assess the long-term impact of sea-level rise on the position of the interface, an additional simulation is considered. The new simulation is identical to the previous one except that the model is run until 2095, to allow for the interface to reach its equilibrium position, while sea level is maintained at an elevation of 0.215 m from 2040 to 2095. The results indicate that the elevation of the freshwater–saltwater interface at the location of the MDDELCC observation well would increase by 3 m after 82 years, which is almost twice as much as the initial simulation where the interface increased by 1.7 m after 28 years (Table 7). This additional simulation suggests that, even if sea level stopped rising in the future, the saltwater–freshwater interface would continue to increase for possibly several decades.

### 5.3. Coastal erosion

Simulated TDS concentrations for the case where the effects of erosion are considered are shown in Fig. 9b. The impact of erosion is most visible close to the shore, where lateral saltwater encroachment occurs between the positions  $x = 240$  m and  $x = 260$  m (Fig. 9b). However, erosion has a minor impact on the vertical position of the saltwater–freshwater interface away from the shore, as shown for the

**Table 7**

Summary of the saltwater–freshwater interface elevation increases at observation wells OW1, MW2, MDDELCC and OW3 for the four scenarios shown in Fig. 10 and the two additional scenarios discussed in the text.

Scenario	Interface elevation increase (m)			
	OW1	OW2	MDDELCC	OW3
Sea level	5.5	2.6	1.7	1.3
Erosion	3.4	1.6	1.0	0.8
Groundwater recharge	1.2	1.6	1.8	1.8
Combined	6.5	4.2	3.5	3.1
Sea-level rise (83 years)	6.1	3.7	3.0	2.5
Groundwater recharge (83 years)	3.3	4.5	5.3	5.7

OW2 (1.6 m), MDDELCC (1.0 m) and OW3 (0.8 m) observation wells in Fig. 10. Erosion will, however, have a greater effect on wells located closer to the sea, as shown in Fig. 10 for the observation well OW1 located at a distance of 50 m from the coast, where the simulated elevation of the interface over the period 2013–2040 is 3.4 m.

#### 5.4. Lower groundwater recharge

Simulated TDS concentrations for the decreased groundwater recharge simulation are shown in Fig. 9c. Compared to the present-day (2013) conditions, the freshwater–saltwater interface would not migrate significantly inland (Fig. 9c). These results suggest that even a significant decrease in recharge would not impact the lateral position of saltwater on a 28-year horizon. However, in Fig. 10, it can be seen that the position of the interface would increase by 1.8 m over the period from 2013 to 2040 m at the MDDELCC observation well (Table 7). The magnitude of the increase in interface elevation is more or less similar regardless of the distance from shore (1.2–1.8 m; Table 7). This increase is related to an average decrease of 6.7 cm in the elevation of the water table.

According to the Ghyben–Herzberg relation, a decrease of 6.7 cm of the water table would induce an increase of the interface of 2.7 m, which is more than the simulated increase of 1.85 m. This difference is mostly due to the fact that the Ghyben–Herzberg theory neglects vertical gradients and assumes hydrostatic conditions, while our simulations are transient, which means that even if the recharge would become constant in 2040 with a value of 151 mm/yr, it would take several more years before the interface reaches a static level. Indeed, an additional simulation where a constant recharge of 151 mm/yr was assigned from 2040 until 2095 shows that the interface would rise three times more in 2095, after 82 years, than after only 28 years. Similarly to the simulations of sea level rise, these simulations with variable recharge show that the freshwater–saltwater interface does not reach its equilibrium position instantaneously after a modification to the aquifer's flow boundaries.

#### 5.5. Combined impacts

Results for the combined impacts of sea-level rise, coastal erosion and decreased groundwater recharge are shown in Fig. 9d. For the MDDELCC observation well, the increase in interface elevation can reach up to 3.5 m while it can reach 6.5 m for well OW1 located 50 m from the coast (Fig. 10 and Table 7). The lateral movement of the interface close to the shore is 37 m.

## 6. Discussion

The water budget computations presented previously suggest that groundwater recharge is expected to slightly increase in the future. However, the variability in predictions is quite high due to the large range of temperatures and precipitation rates predicted by different GCMs for the three scenarios considered. If the worst case climate scenario is used (B1) and if the corresponding model yielding the least precipitation and the highest temperature increase for the area is used, groundwater recharge could be reduced from 220 mm/yr in 2013 to 151 mm/yr for 2040. On the other hand, maximum recharge rates up to 263 mm/yr were also obtained.

Using the worst-case scenario, the climate change simulations in which groundwater recharge is reduced from 220 mm/yr in 2013 to 151 mm/yr in 2040 did not produce a significant impact on the water table and on the position of the freshwater–saltwater interface, since the predicted elevation of the water table decreased by only 6.7 cm and the interface increased by at most 1.8 m.

Coastal erosion also produced minor impacts on the interface, except closer to the sea where the interface was predicted to move inland over a distance of 23 m and its elevation to increase by up to 3.4 m. As can be expected, coastal erosion has a greater impact than decreases in groundwater recharge nearest the coast, by nearly a factor of two. However, further from the sea and close to the groundwater divide, the impact of erosion becomes less than the decrease in recharge, although the impacts are similar (Fig. 10 and Table 7).

Among the three individual impacts of climate change studied, sea-level rise was shown to have the greatest impact on the position of the freshwater–saltwater interface. Sea level rise would increase

the elevation of the interface by up to 5.5 m at 50 m from the coast and up to 1.3 m at a distance of 350 m from the coast. The lateral inland migration of the interface would be 35 m for the 28-year simulation period.

These results contrast with the results of [Green and MacQuarrie \(2014\)](#) who conducted a similar study in New Brunswick in similar types of rocks. As discussed in the introduction, they found that sea-level rise had the least impact on the position of the freshwater–saltwater interface and that a decrease in groundwater recharge was most important. These differences in simulation results are mostly due to the simulation time considered. Green and MacQuarrie conducted their simulations over a 89-year period while our base case simulations were conducted over a 28-year period. However, we also conducted longer simulations that considered a 83-year period. The results for these 83-years simulations are discussed in more detail below, but they show that the dynamics of the groundwater flow system is rather slow and that it takes time for the interface to reach steady state. These simulations also showed that after 83 years, for most of the observation wells, the increase in elevation of the freshwater–saltwater interface became greater for the low groundwater recharge scenario than for the sea-level rise scenario ([Table 7](#)). These results are opposite to those obtained for the 28-years base case simulations ([Table 7](#)), but are more in line with the results obtained by [Green and MacQuarrie \(2014\)](#).

Our results are also consistent with those of [Sherif and Singh \(1999\)](#) who conducted a study on the effects of sea-level rise on the Madras aquifer (India). Although the hydrogeological conditions (hydraulic conductivity, hydraulic gradient) are slightly different from those encountered on the Magdalen Islands, they note that a 0.2 m sea-level rise resulted in a lateral inland displacement of the freshwater–saltwater interface of 36 m, which is consistent with our results. They also observed that changes in the interface are greater near the coast, which is consistent with the results obtained here. [Chang et al. \(2011\)](#) also describe numerical simulations in which they show that sea-level rise has no significant impact on saltwater intrusion in confined and unconfined systems. Under unconfined conditions, the simulated interface moved 128 m inland following a sea-level rise of 4 m. [Ferguson and Gleeson \(2012\)](#) and [Hansen \(2012\)](#) also conclude that coastal aquifers are generally more vulnerable to poor operating practices for drinking water supply than to sea-level changes, although these conclusions have been debated ([Lu et al., 2013](#)).

Municipal pumping wells are not usually located close to the shore because the freshwater–saltwater interface is shallow. Therefore, these types of wells should not be vulnerable to climate change impacts. However, under excessive pumping, the position of the interface can approach the well screen and, because dispersion of the interface caused by pumping can be significant ([Zhou et al., 2005](#)), small vertical movements of the interface could lead to well encroachment. This could be a problem for Grande Entrée Island since the thickness of the freshwater zone is rather small. On the Magdalen Islands, shallow groundwater catchments in the dune areas used for water supply of the local salt mine and for private households would also be most vulnerable to the impact of climate change.

While the impacts of climate change appear to be low for Grande Entrée Island, the 28-year time frame considered in this study is rather short. The time horizon (2040) was mainly chosen according to the study objective, which was to help design a monitoring network that will be operational for the next 30 years. However, a longer period would yield a larger increase in the sea-level rise, more erosion, and possibly even less groundwater recharge, which would in turn result in a greater increase of the elevation of the interface and lateral displacement. Longer simulations that considered a 83-year period showed that even if the climate change impacts become stable after 28 years, the dynamics of the groundwater flow system is such that the interface will continue to increase, up to 2 or 3 times over 28 years, and will require up to 80 years before reaching steady state ([Table 7](#)). These results are consistent with [Webb and Howard \(2011\)](#) who showed that changes to the freshwater–saltwater interface lag behind the equilibrium sea water position during sea-level rise for systems with a high ratio of hydraulic conductivity to recharge and high effective porosity. Notwithstanding the importance of the longer-term simulations, the 28-year simulations were nevertheless important as they highlighted the anticipated climate change effects which may influence the region over the medium term, regardless of the relative change in influence factors at later times.

The simulations showed that the cumulative impacts can be twice those for sea-level rise alone. Although the individual impacts of coastal erosion and lower groundwater recharge are low, their impact is cumulative and it therefore becomes important to consider their combined impact. However, some of the scenarios considered here are quite pessimistic. For example, the rates of coastal erosion used for Grande Entrée Island are much higher than what would normally be expected. In addition, the simulations that assessed changes in recharge were based on the worst case scenario. Therefore, the predictions for interface displacement shown here are probably overestimated.

In light of these results, it is unlikely that the TDEM method has sufficient resolution to measure the expected future increase in elevation of the freshwater–saltwater interface in response to climate change since the anticipated variations are within the uncertainty range of the method. A better alternative to monitor the evolution of the freshwater–saltwater interface would be to use observation wells drilled deeper than the interface. Annual depth-dependent measurements of electrical conductivity would accurately monitor the evolution of the interface and mixing zone. Open-hole conductivity profiles could be obtained with a conductivity probe. However, more precise and reproducible measurements can be achieved with an electromagnetic well log that measures water conductivity within the rock formation within a 1 m radius of the well.

The simulations suggest that the rise of the interface will be highest near the coast and the rise will decrease toward the center of the island. A monitoring well site in the center of the island, on the edge of the watershed, should therefore be avoided since the variations of the interface at that location would be the smallest on the island. However, over the long term, a well too close to the coast may be vulnerable to erosion. In addition, monitoring wells located close to the coast are less representative of private and municipal wells, which are usually located away from the coast to avoid saltwater encroachment. A suitable location for monitoring wells is approximately half the distance between the coast and the center of the island, at a distance of about  $250 \pm 50$  m from the coast. This distance corresponds approximately to the position of the existing MDDELCC observation well. However, using this well as a long-term observation well is not recommended since it will likely be impacted by future municipal wells for which authorization is pending.

### 6.1. Limitations

Seasonal variations in groundwater recharge or sea levels caused by tidal effects, which can also affect saline water intrusion, have not been considered in the simulations. According to [Ataie-Ashtiani et al. \(1999\)](#), tides can cause an increased lateral movement of the interface and yield a more dispersed mixing zone between the salt water and fresh water for unconfined aquifers. [Hansen \(2012\)](#) also mentions that the tide influences the position of the interface.

Another limitation of the study is related to the selected climate change scenarios and the methodology used to represent climate change. Ideally, future periods and reference periods must be at least 30 years apart (e.g., 1961–1990 vs. 2011–2040) to properly assess the impacts of global warming. For the Magdalen Islands, the available climate data do not cover a period of 30 years since the weather station was first installed in 1985, which means that the reference period (1985–2012) is not sufficiently distinct from the period covered by the assessment of climate change. The reference period could therefore already be impacted by climate change, which would yield smaller increases in precipitation and temperature forecasted with the delta change method. The delta change method used for downscaling the GCM data also has some important limitations, the most important of which is that information on the changes in variability and extremes for the predicted climate is lost because the predicted climate relies on observed data ([Van Roosmalen et al., 2007](#)). Moreover, the delta change method also assumes that any biases in the simulation of present-day climate with the GCMs are the same as in the simulation of future climate, while this might not be the case ([Environment Canada, 2014](#)).

Finally, no sensitivity analysis of the individual and combined impacts of climate changes on the position of the interface was conducted and the uncertainties on the predictions were not assessed.

## 7. Conclusions

Numerical simulations were conducted to assess the impact of future climate change on the groundwater resources of the Magdalen Islands. This work was undertaken to support the design of a long-term groundwater monitoring network and for the sustainable management of groundwater resources on the islands.

This study relies mostly on the compilation of existing data, but additional field work has also been carried specifically for this project. Slug tests and groundwater sampling was conducted with pneumatic straddle packers at different depths in a well drilled by the MDDELCC on Grande Entrée Island in the fall of 2012. The salinity profile allowed to directly observe, for the first time on the Magdalen Islands, the depth and shape of the transition zone between freshwater and seawater under natural conditions. This transition zone is located at a depth of 40 m and extends over a thickness of about 10 m.

The impact of climate change on groundwater resources has been assessed for the island of Grande Entrée. Simulations were conducted along a 2D cross-section until 2040 to assess the individual and combined impacts of sea-level rise, coastal erosion and groundwater recharge on the position of the saltwater–freshwater interface. The simulations were performed with the FEFLOW model considering variable-saturation and density-dependent flow and solute transport. The model was driven by observed and projected climate change scenarios for the Magdalen Islands.

The predicted future variation of recharge was determined using the water balance method using the values of precipitation and temperature predicted by GCMs. These values were downscaled using the delta change approach. Predicted future mean recharge rates are slightly higher than actual observations (220 mm/yr), however lower values were used in this study as a worst case scenario.

The simulation results show that among the three impacts considered, the most important is sea-level rise, followed by a decrease in groundwater recharge and coastal erosion. Over a 28-year period, these combined impacts would cause the saltwater–freshwater interface to migrate inland over a distance of 37 m and to vertically increase from 6.5 m near the coast to 3.1 m further inland. While these impacts are rather small for municipal wells located inland, these changes could impact shallow wells located near the coast.

The magnitude of these changes is sufficiently high to be detectable with conductivity probes or electromagnetic well logs in an observation well drilled across the interface. However, time domain electromagnetic surveys would not have sufficient resolution to track them.

## Acknowledgements

We are grateful to the Municipality of Les Îles-de-la-Madeleine for their collaboration on this study, especially Benoit Boudreau and Annick Petitpas for their direct help with the data and field logistics. We are also grateful to Nelly Montcoudiol for her help in the field.

## References

- Ataie-Ashtiani, B., Volker, R.E., Lockington, D.A., 1999. Tidal effects on sea water intrusion in unconfined aquifers. *J. Hydrol.* 216 (1–2), 17–31.
- Bear, J., Cheng, A.H.-D., 2010. *Modeling Groundwater Flow and Contaminant Transport*. Springer, Dordrecht/Heidelberg/London/New York, 834 pp.
- Bernatchez, P., Fraser, C., Friesinger, S., Jolivet, Y., Dugas, S., Drejza, S., et Morissette, A., 2008. *Sensibilité des côtes et vulnérabilité des communautés du golfe du Saint-Laurent aux impacts des changements climatiques (Coastal Sensitivity and Vulnerability of Communities in the Gulf of St. Lawrence to the Impacts of Climate Change)*. Laboratoire de dynamique et de gestion intégrée des zones côtières, Université du Québec à Rimouski, Québec, Canada, 256 pp.
- Bobba, A.G., 2002. Numerical modelling of salt-water intrusion due to human activities and sea-level change in the Godavari Delta, India. *Hydrol. Sci.* 47(S), S67–S80.
- Brisebois, D., 1981. *Lithostratigraphie des strates permo-carbonifères de l'archipel des Îles de la Madeleine (Lithostratigraphy of the Permo-Carboniferous Strata of the Magdalen Islands)*. Ministère de l'énergie et des ressources du Québec.
- Bureau d'audience publique dur l'environnement (BAPE), 2013. *Les effets liés à l'exploration et l'exploitation des ressources naturelles sur les nappes phréatiques aux îles de la Madeleine, notamment ceux liés à l'exploration et l'exploitation gazière (Effects related to the exploration and exploitation of natural resources on groundwater to the Magdalen Islands, including those related to the exploration and gas development)*. Rapport d'enquête et d'audiences publiques, 207 pp.

- Chang, S.W., Clement, T.P., Simpson, M.J., Lee, K., 2011. Does sea-level rise have an impact on saltwater intrusion? *Adv. Water Resour.* 34, 1283–1291.
- Chouteau, M., Bouchedda, A., Madani, A., 2011. Développement d'une méthodologie de suivi de l'impact des changements climatiques sur les eaux souterraines pour les Îles-de-la-Madeleine. Phase 2 : Caractérisation des sites, détermination des profils de références et de la méthodologie de suivi (Development of a Methodology for Monitoring the Impact of Climate Change on Groundwater in the Magdalen Islands. Phase 2: Site Characterization, Determination of Reference Profiles and Monitoring Methodology). École Polytechnique de Montréal, Québec, Canada.
- Comte, J., Banton, O., 2006. Modelling of Seawater Intrusion in the Magdalen Islands (Quebec, Canada). In: Proceedings of the 1st SWIM-SWICA Joint Saltwater Intrusion Conference, Cagliari-Chia Laguna, Italy, September 24–29, 2006, pp. 303–310.
- Comte, J., Banton, O., 2007. Cross-validation of geo-electrical and hydrogeological models to evaluate seawater intrusion in coastal aquifers. *Geophys. Res. Lett.* 34, L10402.
- Daigle, R.J., 2011. Sea-level rise estimates for New Brunswick municipalities. Report prepared by R.J. Daigle Enviro for the Atlantic Climate Adaptation Solutions Association. [www.atlanticadaptation.ca/node/203](http://www.atlanticadaptation.ca/node/203) (accessed 01.12.14).
- Dagan, G., Bear, J., 1968. Solving the problem of interface upconing in a coastal aquifer by the method of small perturbations. *J. Hydraul. Res.* 6 (1), 15–44.
- Dessureault, R., Simard, G., 1970. Hydrogéologie des îles de la Madeleine (Hydrogeology of the Magdalen Islands). Gouvernement du Québec, Ministère des Richesses naturelles, 106 pp.
- DHI-WASY, 2013. FEFLOW finite element subsurface flow and transport simulation system—user's manual/reference manual/white papers, Version 6.1. Technical Report. DHI-WASY GmbH, Berlin.
- Dietrich, J., Lavoie, D., Hannigan, P., Pinet, N., Castonguay, P., Giles, P., Hamblin, A.P.A.P., 2011. Geological setting and resource potential of conventional petroleum plays in Paleozoic basins in eastern Canada. *Bull. Can. Petrol. Geol.* 59, 54–84.
- Environment Canada, 2014. Canadian Climate Change Scenarios Network. [www.cccsn.ec.gc.ca/?page=scen-intro](http://www.cccsn.ec.gc.ca/?page=scen-intro) (accessed May 2014).
- Ferguson, G., Gleeson, T., 2012. Vulnerability of coastal aquifers to climate change and groundwater use. *Nat. Clim. Change* 2, 342–345. <http://dx.doi.org/10.1038/nclimate1413>.
- Fisheries and Oceans Canada, 2014. Canadian Tides and Water Levels Data Archive. <http://www.isdm-gdsi.gc.ca/isdm-gdsi/twl-mne/index-eng.htm#s5> (accessed April 2014).
- Forbes, D.L., Parkes, G.S., Manson, G.K., Ketch, L.A., 2004. Storms and shoreline retreat in the southern Gulf of St. Lawrence. *Mar. Geol.* 210 (1–4), 169–204.
- Gelhar, L.W., Axness, C.L., 1983. Three-dimensional stochastic analysis of macrodispersion in aquifers. *Water Resour. Res.* 19, 161–180.
- Gélinas, P.J., Choquette, M., 1996. Essais de caractérisation des grès rouges de Cap-aux-Meules (Characterization of the Red Sandstones of Cap-aux-Meules). Groupe de recherche en environnement et en Géo-Ingénierie, Département de géologie et génie géologique, Université Laval, Québec, Canada.
- Government of Québec, 2008. Québec and climate change, a challenge for the future, 2006–2012 action plan. [www.mdefp.gouv.qc.ca/changements/plan\\_action/2006-2012\\_en.pdf](http://www.mdefp.gouv.qc.ca/changements/plan_action/2006-2012_en.pdf)
- Green, N.R., MacQuarrie, K.T.B., 2014. An evaluation of the relative importance of the effects of climate change and groundwater extraction on seawater intrusion in coastal aquifers in Atlantic Canada. *Hydrogeol. J.* 22, 609–623.
- Hansen, B.A., 2012. Simulating the Effects of Climate Change on a Coastal Aquifer, Summerside, Prince Edward Island. Department of Earth Science, Saint Francis Xavier University, Nova Scotia.
- Healy, R.W., 2010. Estimating Groundwater Recharge. Cambridge University Press, Cambridge, UK.
- IPCC, 2007. Climate change 2007: impacts, adaptation and vulnerability. In: Parry, M.L., Canziani, O.F., Palutikof, J.P., van der Linden, P.J., Hanson, C.E. (Eds.), Contribution of Working Group II to the Fourth Assessment Report of the Intergovernmental Panel on Climate Change. Cambridge University Press, Cambridge.
- Koohzare, A., Vanicek, P., Santos, M., 2008. Pattern of recent vertical crustal movements in Canada. *J. Geodyn.* 45, 133–145.
- Leblanc, Y., (M.Sc. thesis) 1994. Analyse et modélisation numérique de huit puits de production sur l'île de Cap-aux-Meules, Îles-de-la-Madeleine (Analysis and Numerical Modeling of Eight Production Wells on the Island of Cap-aux-Meules, Magdalen Islands). Université Laval, Québec, Canada.
- Lu, C., Werner, A.D., Simmons, C.T., 2013. Threats to coastal aquifers. *Nat. Clim. Change* 3, 605.
- Madelin'Eau, 2009. Secteur de Grande-Entrée – Flanc Nord, Alimentation en eau potable; Demande d'autorisation en vertu de l'article 31 du règlement sur le captage des eaux souterraines; Puits de production GE-09-01A, GE-09-02, GE-09-03, GE-09-04 et GE-09-05; Municipalité des îles de la Madeleine (Grande-Entrée area – North Flank, drinking water supply; Application for authorization under Article 31 of the Regulation on groundwater abstraction; Production wells GE-09-01A, GE-09-02, GE-09-03, GE-09-04 et GE-09-05; Municipality of the Magdalen Islands). Québec, July 2009.
- Morgan, L.K., Werner, A.D., 2014. Seawater intrusion vulnerability indicators for freshwater lenses in strip islands. *J. Hydrol.* 508, 322–327. <http://dx.doi.org/10.1016/j.jhydrol.2013.11.002>.
- Poulin, M., 1977. Étude hydrogéologique des îles de Grosse-Île et de Grande-Entrée Îles-la-Madeleine (Hydrogeological study of the Grosse-Île and Grande Entrée Islands, Magdalen islands). Service des eaux souterraines, Ministère des richesses naturelles, Gouvernement du Québec.
- Schulze-Makuch, D., 2005. Longitudinal dispersivity data and implications for scaling behavior. *Ground Water* 43 (3), 443–456.
- Sherif, M.M., Singh, V.P., 1999. Effect of climate change on sea water intrusion in coastal aquifers. *Hydrol. Process.* 13 (8), 1277–1287.
- Stammer, D., Cazenave, A., Ponte, R.M., Tamisieva, M.E., 2013. Causes for contemporary regional sea level changes. *Ann. Rev. Mar. Sci.* 5, 21–46.
- Tang, D.H., Frind, E.O., Sudicky, E.A., 1981. Contaminant transport in fractured porous media: analytical solution for a single fracture. *Water Resour. Res.* 17 (3), 555–564.
- Sylvestre, M., 1979. Carte hydrogéologique des îles de la Madeleine (Hydrogeological map of the Magdalen Islands). Gouvernement du Québec, Ministère des Richesses naturelles, Direction générale des eaux. Service des eaux souterraines.
- Thorntwaite, C.W., 1948. An approach toward a rationale classification of climate. *Geograph. Rev.* 38, 55–94.
- Thorntwaite, C.W., Mather, J.R., 1955. The water balance. *Publ. Climatol. Lab. Climatol. Drexel Inst. Technol.* 8 (1), 1–104.

- Van Genuchten, M.Th., 1980. A closed-form equation for predicting the hydraulic conductivity of unsaturated soils. *Soil Sci. Soc. Am. J.* 44 (5), 892–898.
- Van Roosmalen, L., Christensen, B.S.B., Sonnenborg, T.O., 2007. Regional differences in climate change impacts on groundwater and stream discharge in Denmark. *Vadose Zone J.* 6 (3), 554–571.
- Vasseur, L., Catto, N., 2008. Atlantic region. In: Lemmen, D.S., Warren, F.J., Lacroix, J., Bush, E. (Eds.), *National Climate Change Assessment*. Government of Canada, Ottawa, 52 pp. (Chapter 4).
- Vermeer, M., Rahmstorf, S., 2009. Global sea level linked to global temperature. *Proc. Natl. Acad. Sci.* 106 (51), 21527–21532.
- Webb, M.D., Howard, K.W.F., 2011. Modeling the transient response of saline intrusion to rising sea-levels. *Ground Water* 49 (4), 560–569, <http://dx.doi.org/10.1111/j.1745-6584.2010.00758.x>.
- Werner, A.D., Simmons, C.T., 2009. Impact of sea-level rise on sea water intrusion in coastal aquifers. *Ground Water* 47 (2), 197–204, <http://dx.doi.org/10.1111/j.1745-6584.2008.00535.x>.
- Werner, A.D., Ward, J.D., Morgan, L.K., Simmons, C.T., Robinson, N.I., Teubner, M.D., 2012. Vulnerability indicators of seawater intrusion. *Ground Water* 50 (1), 48–58, <http://dx.doi.org/10.1111/j.1745-6584.2011.00817.x>.
- Zhou, Q., Bear, J., Bensabat, J., 2005. Saltwater upconing and decay beneath a well pumping above an interface zone. *Trans. Porous Media* 61, 337–363, <http://dx.doi.org/10.1007/s11242-005-0261-4>.